

On the Mellor–Yamada Turbulence Closure Scheme: The Surface Boundary Condition for q^2

MICHAEL W. STACEY

Department of Physics, Royal Military College of Canada, Kingston, Ontario, Canada

STEPHEN POND

Department of Oceanography, The University of British Columbia, Vancouver, British Columbia, Canada

(Manuscript received 21 April 1995, in final form 21 June 1996)

ABSTRACT

A numerical model that uses a level-2½ turbulence closure scheme is used to compare two boundary conditions for the turbulent energy at the air–sea interface. One boundary condition, the most commonly used, sets the turbulent kinetic energy proportional to the friction velocity squared, while the other sets the vertical diffusive flux of turbulent kinetic energy proportional to the friction velocity cubed. The first boundary condition arises from consideration (simplification) of the turbulence closure scheme near boundaries, and the second arises from consideration of the influence of surface gravity waves on the transfer of turbulent kinetic energy from the wind to the water. Simulations using these two boundary conditions are compared to month-long observations of velocity, temperature, and salinity (as shallow as 2 m from the surface) from Knight Inlet, British Columbia, Canada. The circulation in the inlet is strongly influenced by the wind, tides, and freshwater runoff. The two boundary conditions produce simulations that are different down to a depth of at least 5 m. Somewhat more accurate simulations are produced by the second boundary condition. Also, simulations using the second boundary condition are more sensitive to variations in the roughness length. Based on the simulations, roughness lengths as large as 1 m (or greater) are possible.

1. Introduction

Two-dimensional (laterally integrated) numerical models are capable of simulating realistically much of the circulation in long, narrow fjords (e.g., Lavelle et al. 1991; Stacey and Pond 1992; Stacey et al. 1995). A recent model of Knight Inlet (Stacey et al. 1995) simulates the circulation caused by the combined influences of the winds, tides, and freshwater input. The model was used to simulate the circulation during two 30-day time periods: a period of low freshwater runoff during the spring of 1988 and a period of high freshwater runoff during the summer of 1989. Observations of velocity, temperature, and salinity (at depths as shallow as 2 m) during these time periods documented the circulation (Baker and Pond 1995). By allowing the numerical grid of the model to move up and down with the tide, very fine resolution near the surface could be attained, so the circulation at 2-m depth (and shallower) could be simulated. The model simulated the observations quite well, but there was a tendency for the velocity to be quite

surface-intensified at depths less than the shallowest observations. Although this predicted surface intensification cannot be discounted by the observations, it runs counter to intuitive expectations for the region close to the surface where the breaking of surface waves as well as shear-generated turbulence presumably can cause significant mixing.

Turbulent mixing is incorporated into the model by employing a level 2½ turbulence closure scheme (Mellor and Yamada 1982). With this scheme, the vertical diffusion coefficients are proportional to the product of a velocity scale q (which is calculated from the turbulent kinetic energy density $\rho q^2/2$, where ρ is the water density) and a length scale l . The length scale is prescribed, taking the form (when the roughness length z_0 is included)

$$l = k(\bar{z} + z_0) \quad (1)$$

near the surface (bottom), where $k = 0.4$ is von Kármán's constant and \bar{z} is the distance from the surface (bottom). The turbulent kinetic energy, on the other hand, is calculated from a differential equation, so boundary conditions are required for it. Stacey et al. (1995), following Mellor and Yamada (1982), use

$$q^2 = B_l^{2/3} u_*^2 \quad (2)$$

Corresponding author address: Dr. Michael W. Stacey, Department of Physics, Royal Military College of Canada, Kingston, ON K7K 5L0, Canada.
E-mail: stacey-m@rmc.ca

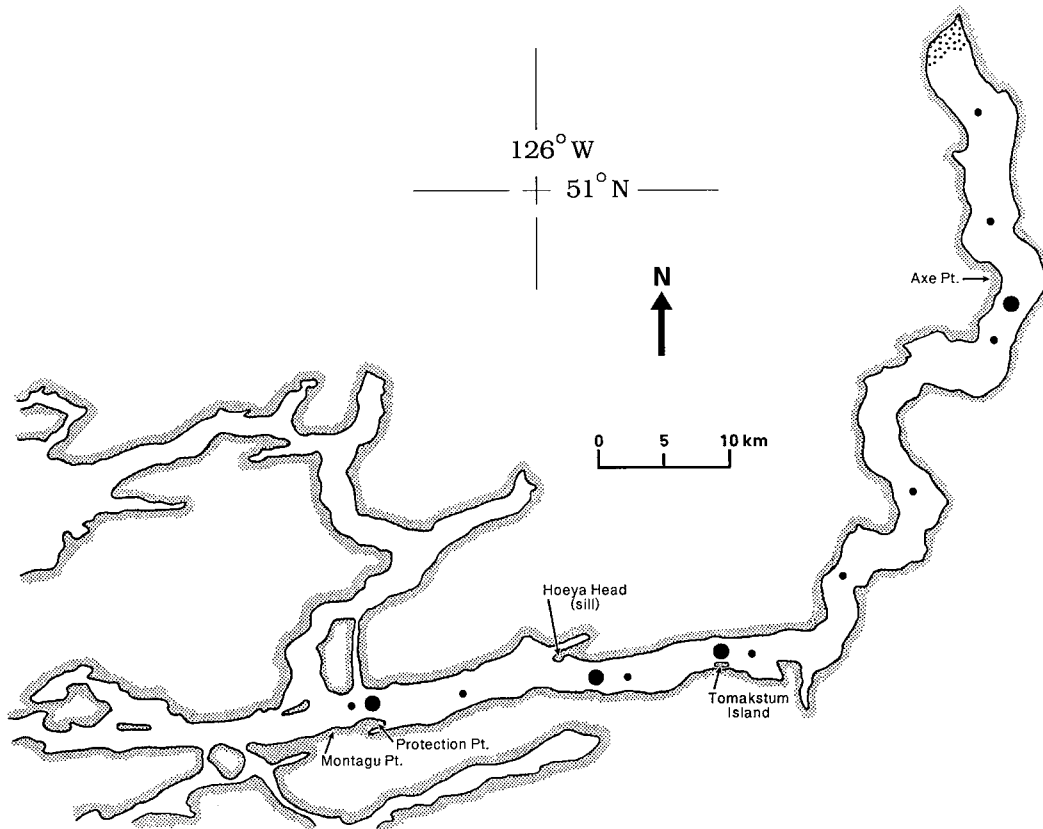


FIG. 1. Plan view of Knight Inlet (from Stacey et al. 1995). The large, solid circles indicate the locations where moorings were deployed. The small, solid circles indicate CTD stations. At the moorings close to Tomakstum Island and Protection Point, observations were made as shallow as 2 m from the surface.

as the surface boundary condition, where $B_s = 16.6$ and u_* is the friction velocity for the water. This boundary condition is commonly used (e.g., Blumberg and Mellor 1987) and is obtained from assuming that the production and dissipation rate of turbulent energy are equal near the surface. Alternatively, based on consideration of the wave-enhanced turbulence in the surface layer, the level $2\frac{1}{2}$ turbulence closure scheme has also been used with the surface boundary condition (Craig and Banner 1994)

$$\lambda_v \frac{\partial}{\partial z} \left(\frac{q^2}{2} \right) = \alpha u_*^3, \quad (3)$$

where λ_v is the vertical diffusion coefficient for turbulent kinetic energy and α is a constant, set equal to 100 by Craig and Banner. Since this boundary condition is obtained from an explicit consideration of the influence of the wave field on the water, one might expect models that use it to give better simulations, at least near the surface where wave forcing can be very important.

In this paper, simulations using the two surface boundary conditions, (2) and (3), are compared by using them with the model of Stacey et al. (1995) to simulate the circulation in Knight Inlet. Simulations using the

first boundary condition have already been presented by Stacey et al. (1995) for the case where the roughness length $z_0 = 0$ m. Here, simulations where $z_0 = 0.1$ m and 1 m are also considered. Craig and Banner (1994) found that roughness lengths up to 1 m (or greater) appear to be possible, so we will also investigate the influence that the roughness length has on the near-surface flow.

2. Background

a. The data

Moorings were deployed in March 1988 (during a period of low runoff) and in June 1989 (during a period of high runoff) for approximately one month in Knight Inlet (Fig. 1). CTD surveys were also conducted. Details about the data can be found in Baker (1992), Baker and Pond (1995), and Stacey et al. (1995). Observations of velocity, salinity, and temperature were made near the surface during both periods at Protection Point and Tomakstum Island, where S4 current meters were deployed from floats at depths of 2, 4, 6, 9, and 12 m. The data from Protection Point were used to force the model at its open boundary; however, the data from Tomakstum

Island are completely independent of the model and can therefore be used to investigate the performance of the model close to the surface. Below 12 m, Cyclesonde profiling current meters and Anderaa current meters were used. The water depth at Tomakstum Island (Protection Point) is about 350 m (200 m).

Winds were observed at Protection Point and Tomakstum Island. Stacey et al. (1995) found that a spatially uniform wind field using only the winds from Tomakstum Island produced more accurate simulations of the circulation than a wind field varied spatially between Tomakstum Island and Protection Point. The results discussed below were produced using the spatially uniform wind field.

The Klinaklini and Franklin Rivers at the head of Knight Inlet, the major sources of freshwater input, are gauged, and the harmonic constants for the major tidal constituents are known from previous tidal height measurements.

b. The model

Laterally averaged equations of motion have been used to successfully simulate the circulation in Knight Inlet (see Stacey et al. 1995 for details). The turbulent kinetic energy, which is the focus of attention in this paper, is used to determine the vertical eddy diffusion coefficients A_v , K_v , and λ_v for momentum, heat, and turbulent energy respectively; that is,

$$\begin{aligned} A_v &= S_M l q \\ K_v &= S_H l q \\ \lambda_v &= S_q l q, \end{aligned} \quad (4)$$

where S_M , S_H , and S_q are dimensionless stability-dependent parameters (Mellor and Yamada 1982) and l is the length scale prescribed here as

$$\begin{aligned} l &= 0.105(H + \eta) \operatorname{erf} \left[\frac{k}{0.105} \frac{\sqrt{\pi}}{2} \frac{(H - z)}{(H + \eta)} \right] \\ &\times \operatorname{erf} \left[\frac{k}{0.105} \frac{\sqrt{\pi}}{2} \frac{(z + z_0 + \eta)}{(H + \eta)} \right]. \end{aligned} \quad (5)$$

The only difference between the l given here and the l used by Stacey et al. (1995) is the inclusion here of the roughness length z_0 near the surface. Note that (5) reduces to (1) both near the bottom located at $z = H$ [taking into consideration that z_0 is not accounted for in (5) near the bottom] and near the surface located at $z = -\eta$.

A lower bound,

$$K_{V_{\min}} = A_{V_{\min}} = a_0 N^{-\beta}, \quad (6)$$

where $a_0 = 3.1 \times 10^{-4} \text{ cm}^2/\text{s}^{5/2}$, $\beta = 1.5$, and N is the Brunt-Väisälä frequency, was placed on A_v and K_v to obtain accurate simulations well away from boundaries.

The vertical spacing between the grid points in the

model increases away from the surface. There are 5 (14) grid points within about 2 m (10 m) of the surface. The horizontal spacing between the grid points is also variable, increasing in both directions away from the sill of the inlet. In the region of the mooring at Tomakstum Island, where the model is compared to the observations, the grid points are less than 1 km apart. In this paper, model data from columns 16, 17, and 18 (15, 16, and 17) for the alongchannel velocity (density) are compared to the observations. These columns straddle the location of the mooring. Different columns are used for the velocity and density because the model uses a staggered grid.

The bottom slope varies significantly along the inlet, and in the region of the sill it is large by oceanographic standards. Because sigma coordinates can cause numerical models to produce inaccurate simulations near regions of steep topography (e.g., Haney 1991), the vertical z coordinate was transformed to \hat{z} using the quasi-Cartesian transformation

$$\frac{\hat{z}}{H} = \frac{z + \eta}{H + \eta}. \quad (7)$$

Since $|\eta/H| \ll 1$, one sees that $\hat{z} \approx z$ except near the surface; hence the term quasi-Cartesian. Note, however, that $\hat{z} = 0$ at the surface (i.e., the upper bound on \hat{z} is not a function of η) so the vertical resolution of the numerical model near the surface is not constrained by the range over which η varies.

3. Comparisons

In the comparisons that follow, changes are made only to the surface boundary condition on q^2 [using either (2), the boundary condition of Mellor and Yamada (1982), or (3), the boundary condition of Craig and Banner (1994)] and/or to the value used for the roughness length. Visually, the simulated time series of velocity and sigma-t for the different model runs at 2-m depth and deeper at Tomakstum Island are similar (see Stacey et al. 1995 for examples). However, when the basic statistics of the time series are calculated, differences become apparent.

The data were low-pass filtered with a 25-h running mean to remove most of the tidal energy at diurnal frequencies and higher. This filter is applied because the Craig and Banner boundary condition arises from a consideration of the wind-forced motion, and the lower frequencies will in a relative sense contain more wind-forced energy. However, there is obviously tidal energy at the lower frequencies also; thus, the wind- and tidally forced motions cannot be separated completely. Another reason for applying the low-pass filter is that one expects diffusive processes to have more influence on the circulation at lower frequencies.

The variances (with the means removed) and the means of velocity and sigma-t time series over the top

TABLE 1. Variances of velocity and sigma-t time series (*varu*, for velocity; *vars* for sigma-t). Model column 16 (17) is used for sigma-t (velocity).

(a) Observations (Tomakstum Island)						
(i) 1988			(ii) 1989			
Depth (m)	<i>varu</i> (cm ² s ⁻²)	<i>vars</i>	Depth (m)	<i>varu</i> (cm ² s ⁻²)	<i>vars</i>	
2	287	.97	2	632	14.5	
4	136	.48	4	165	10.7	
6	59	.19	6	58	3.4	

(b) Model [Mellor and Yamada (1982) boundary condition]						
(i) 1988						
Depth (m)	<i>z</i> ₀ = 0 m		<i>z</i> ₀ = 0.1 m		<i>z</i> ₀ = 1 m*	
	<i>varu</i> (cm ² s ⁻²)	<i>vars</i>	<i>varu</i> (cm ² s ⁻²)	<i>vars</i>	<i>varu</i> (cm ² s ⁻²)	<i>vars</i>
2	573	.49	593	.47		
4	334	.25	347	.25		
6	187	.11	196	.10		

(ii) 1989						
2	853	20.9	844	21.1	842	20.5
4	274	7.0	274	7.0	285	6.9
6	161	2.3	149	2.2	157	2.1

(c) Model [Craig and Banner (1994) boundary condition]						
(i) 1988						
2	525	.57	506	.59	359	.43
4	340	.29	334	.30	321	.31
6	190	.11	192	.12	208	.15

(ii) 1989						
2	677	23.9	660	23.9	559	19.9
4	231	7.1	236	7.1	259	7.8
6	147	1.7	150	1.8	155	1.9

* The MYBC went unstable in 1988.

6 m of the water column at Tomakstum Island are calculated. Also, the sum of the squares of the residuals (with the mean removed and divided by the number of data points) between the simulated and observed data are calculated.

a. The variances

The Craig and Banner boundary condition (CBBC) produces velocity variances at 2-m depth closer than those of the Mellor–Yamada boundary condition (MYBC) to those of the observations (Table 1). When *z*₀ = 0 m, both the CBBC and the MYBC overestimate the velocity variance at 2 m in 1988, but when *z*₀ = 1 m, the CBBC produces a variance at 2 m that is noticeably closer to that of the observations, while the MYBC causes the model to go unstable. At 6-m depth, the MYBC and the CBBC have velocity variances that are about the same, and both are larger than the observed variances.

The sigma-t variances in 1988, for both the model and the data, are small relative to the means (Table 2) and the sum of the squares of the residuals (Table 3). Consequently, the small changes in the variances be-

TABLE 2. Means of the velocity and sigma-t time series.

(a) Observations (Tomakstum Island)						
(i) 1988			(ii) 1989			
Depth (m)	Velocity (cm s ⁻¹)	Sigma-t	Depth (m)	Velocity (cm s ⁻¹)	Sigma-t	
2	-11.5	21.0	2	-21.2	9.7	
4	-6.5	21.8	4	-7.8	14.6	
6	-3.2	22.7	6	-2.6	18.7	

(b) Model [Mellor and Yamada (1982) boundary condition]						
(i) 1988						
Depth (m)	<i>z</i> ₀ = 0 m		<i>z</i> ₀ = 0.1 m		<i>z</i> ₀ = 1 m*	
	Velocity (cm s ⁻¹)	Sigma-t	Velocity (cm s ⁻¹)	Sigma-t	Velocity (cm s ⁻¹)	Sigma-t
2	-6.1	22.4	-6.1	22.4		
4	-2.8	22.9	-2.8	22.9		
6	-.6	23.2	-.6	23.2		

(ii) 1989						
2	-16.9	13.6	-16.8	13.6	-17.7	13.7
4	-2.2	17.8	-1.9	17.8	-3.0	17.7
6	3.5	20.0	3.4	19.9	3.0	19.9

(c) Model [Craig and Banner (1994) boundary condition]						
(i) 1988						
2	-7.9	22.5	-8.1	22.5	-9.2	22.6
4	-6.0	22.8	-6.7	22.8	-8.5	22.5
6	-2.9	23.1	-4.0	23.1	-6.1	23.0

(ii) 1989						
2	-19.1	12.2	-19.5	12.3	-21.4	13.6
4	-3.0	16.5	-2.7	16.4	-8.5	16.1
6	4.3	19.6	4.2	19.5	3.0	18.9

* The MYBC went unstable in 1988.

tween model runs are not meaningful. In all cases, the model produces variances that are less than those of the data, but this discrepancy could be caused by nothing more than, for example, small errors in the initialization of the density field.

The sigma-t variances in 1989 were much larger than they were in 1988 (because the freshwater runoff in June 1989 was much larger than in March 1988) and both boundary conditions cause overestimates of the variance at 2-m depth and underestimates of the variance at 4- and 6-m depths.

b. The means

The CBBC produces mean values closer than those of the MYBC to those of the observations (Table 2). To illustrate this point for the case where *z*₀ = 0 m, Fig. 2 shows the mean velocity in 1988 (calculated by doing a harmonic analysis on the data), and Fig. 3 shows the mean sigma-t in 1989. The profiles for the three model columns closest to the mooring location are shown so that the variability between the columns can be appreciated.

TABLE 3. Sum of the square of the residuals between the simulated and observed time series, divided by the number of data points (696). SSRV, for velocity; SSRS for sigma-t).

(a) Mellor and Yamada (1982) boundary condition						
(i) 1988						
Depth (m)	$z_0 = 0$ m		$z_0 = 0.1$ m		$z_0 = 1$ m*	
	SSRV ($\text{cm}^2 \text{s}^{-2}$)	SSRS	SSRV ($\text{cm}^2 \text{s}^{-2}$)	SSRS	SSRV ($\text{cm}^2 \text{s}^{-2}$)	SSRS
2	369	1.8	396	1.8		
4	281	1.0	292	1.0		
6	188	.41	190	.39		
(ii) 1989						
2	509	13.7	495	13.0	475	13.7
4	254	5.3	241	5.1	261	5.2
6	108	2.2	98	2.5	110	2.2
(b) Craig and Banner (1994) boundary condition						
(i) 1988						
2	307	2.0	306	2.1	237	2.0
4	241	1.1	233	1.2	213	1.2
6	158	.50	160	.51	158	.58
(ii) 1989						
2	333	19.8	327	19.8	298	17.0
4	232	10.2	234	9.5	234	10.0
6	117	3.3	124	3.5	129	2.8

* The MYBC went unstable in 1988.

c. The residuals

At 2-m depth for velocity, the CBBC produces residual variances that are, in all cases, smaller than those of the MYBC (Table 3). For 1988, the CBBC produces its smallest residuals at all three depths when $z_0 = 1$ m. This result suggests that large roughness lengths are indeed a possibility. At 4-m and 6-m depths (Table 3),

the CBBC and MYBC produce residuals that are about the same.

For sigma-t in 1988, the residual variances are much larger than the variances of the observations (Table 2) and cannot reasonably be used to compare the relative merits of the CBBC and the MYBC. For sigma-t in 1989, the MYBC gives residuals that are marginally smaller than those of the CBBC at 2-m and 6-m depths and about half the size of those of the CBBC at 4-m depth.

4. Discussion and conclusions

A numerical model of Knight Inlet that uses the Mellor–Yamada level $2\frac{1}{2}$ turbulence closure scheme has been used to test two surface boundary conditions for the turbulent kinetic energy. Simulations produced by the boundary conditions of Mellor and Yamada (1982) and Craig and Banner (1994) have been compared to observations made near the surface of the inlet during two month-long periods, in the spring of 1988 and in the summer of 1989. The comparisons have been made by calculating the variances and means of the simulated and observed velocity and sigma-t, and by calculating the sum of the squares of the residuals between the simulated and observed values at depths 2, 4, and 6 m.

Overall, the Craig and Banner boundary condition has been found to produce marginally better simulations. Close to the surface, that is, at 2-m depth, and for velocity the Craig and Banner boundary condition clearly produces better simulations. For sigma-t, the 1988 data are of no use in determining which boundary condition is better. For 1989, the mean sigma-t profile is better simulated by the Craig and Banner boundary condition,

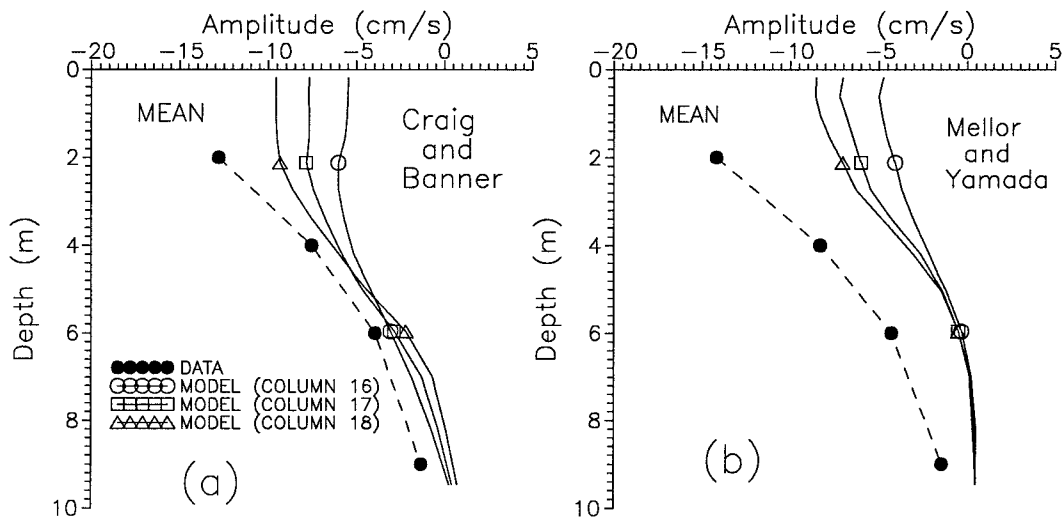


FIG. 2. The mean alongchannel velocity near Tomakstum Island in 1988, over the upper 10 m: (a) simulated profiles for the case where the Craig and Banner (1994) boundary condition is used and (b) simulated profiles for the case where the Mellor and Yamada (1982) boundary condition is used. In both cases, $z_0 = 0$ m. The mean observed velocity is plotted in both (a) and (b). To reduce clutter, not every model grid point is labeled.

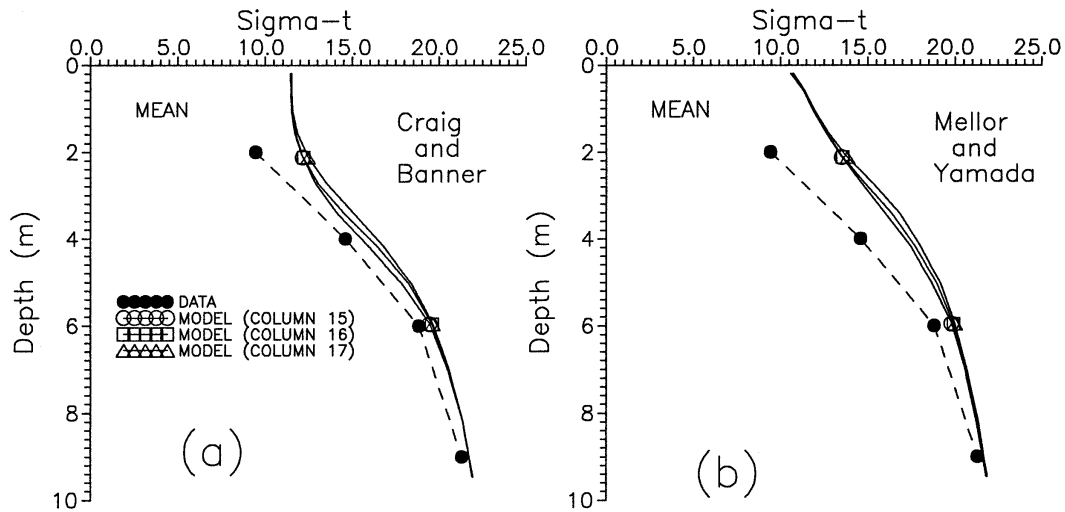


FIG. 3. As in Fig. 2 but for sigma-t in 1989.

while the residuals are smaller for the Mellor–Yamada boundary condition. The mean velocity profile is better simulated by the Craig and Banner boundary condition.

The Craig and Banner boundary condition gives simulations that, for 1988 in particular, are sensitive to variations in the roughness length. Roughness lengths at least as large as 1 m appear possible. Values for the roughness length larger than 1 m were not examined because it would be questionable how to interpret simulated data that were from a depth z less than the z_0 used for the roughness length. Also, because the wind and, therefore, the sea state are varying with time, the roughness length should in principal also vary with time. Attempts have been made to parameterize the roughness length, as discussed by Craig and Banner (1994), but it remains a difficult quantity to determine. The Craig and Banner boundary condition depends directly on the roughness length through its dependence on λ_v [see Eqs. (3) and (4)], so one would expect simulations that use it to be more sensitive to changes in the roughness length than those that use the Mellor–Yamada boundary condition.

The sum of the squares of the residuals is never less than about half the variance in the individual time series; hence there is much room for improvement. However, much of this improvement may only be attainable through better knowledge of the inputs, such as the wind field. Given that much of the residual is likely caused by factors other than the surface boundary condition used for q^2 , it is noteworthy that an improvement in the simulation is detectable when the Craig and Banner boundary condition is used, and thus it is likely the better boundary condition to use, at least when modeling wind-forced flows in inlets.

As a final point, even when the low-pass filter is not

applied, the residual variances tend to be somewhat smaller when the Craig and Banner boundary condition is used, and a number of tidal constituents (the M_2 sigma-t in 1989, for example) are noticeably better simulated. Also, the surface intensification noted by Stacey et al. (1995) is reduced, presumably because the Craig and Banner boundary condition directly influences the vertical diffusion rate of q^2 and therefore enhances the rate at which energy penetrates to depth.

REFERENCES

- Baker, P. D., 1992: Low frequency residual circulation in Knight Inlet, a fjord of coastal British Columbia. M.S. thesis, Dept. of Earth and Ocean Sciences, University of British Columbia, 184 pp.
- , and S. Pond, 1995: The low-frequency residual circulation in Knight Inlet, British Columbia. *J. Phys. Oceanogr.*, **25**, 747–763.
- Blumberg, A. F., and G. L. Mellor, 1987: A description of a three-dimensional coastal ocean circulation model. *Three-Dimensional Coastal Ocean Models*, N. S. Heaps, Ed., American Geophysical Union, 1–16.
- Craig, P. D., and M. L. Banner, 1994: Modeling wave-enhanced turbulence in the ocean surface layer. *J. Phys. Oceanogr.*, **24**, 2546–2559.
- Haney, R. L., 1991: On the pressure gradient force over steep topography in sigma coordinate ocean models. *J. Phys. Oceanogr.*, **21**, 610–619.
- Lavelle, J. W., E. D. Cokelet, and G. A. Cannon, 1991: A model study of density intrusions into and circulation within a deep, silled estuary: Puget Sound. *J. Geophys. Res.*, **96**, 16 779–16 800.
- Mellor, G. L., and T. Yamada, 1982: Development of a turbulence closure model for geophysical fluid problems. *Rev. Geophys. Space Phys.*, **20**, 851–875.
- Stacey, M. W., and S. Pond, 1992: A numerical model of the internal tide in Knight Inlet, British Columbia. *Atmos.–Ocean*, **30**, 383–418.
- , —, and Z. P. Nowak, 1995: A numerical model of the circulation in Knight Inlet, British Columbia, Canada. *J. Phys. Oceanogr.*, **25**, 1038–1062.